Effect of the duration of a wet KCN etching step and post deposition annealing on the efficiency of $Cu_2ZnSnSe_4$ solar cells

M. Sylvester[2,3,4], Guy Brammertz[1,2], Bart Vermang[3,4], Samaneh Ranjbar[2,3,5] Marc Meuris[1,2], Jef Vleugels[6] and Jef Poortmans[2,3,4]

[1]imec division IMOMEC - partner in Solliance, Wetenschapspark 1, 3590 Diepenbeek, Belgium

[2] Institute for Material Research (IMO) Hasselt University, Wetenschapspark 1, 3590 Diepenbeek, Belgium

[3] imec- partner in Solliance, Kapeldreef 75, 3001 Leuven, Belgium

[4] Department of Electrical Engineering (ESAT), KU Leuven, Kasteelpark Arenberg 10, 3001 Heverlee, Belgium

[5] I3N - Departamento de Física, Universidade de Aveiro, Campus Universitário de Santiago, 3810-193 Aveiro, Portugal.

[6] Department of Materials Engineering (MTM), KU Leuven, Kasteelpark Arenberg 44, 3001 Heverlee, Belgium

The influence of the duration of the KCN etching step on the efficiency of $Cu_2ZnSnSe_4$ (CZTSe) solar cells and Post deposition annealing (PDA) has been explored. CZTSe thin film absorbers prepared by selenization at 450ºC were etched by 5wt% KCN/KOH from 30s up to 360s before solar cell processing. KCN etching times above 120s resulted in poor efficiencies. The fill factor (FF) and short circuit current density (Jsc) of these devices were affected severely. After annealing the solar cells at 200°C in N_2 atmosphere the best devices degraded and poor devices improved. Combined physical and optoelectronic characterization of the solar cells showed that PDA modifies the bulk defect density and also surface composition which reflects in the solar cell performance.

1). Introduction

Kesterite $Cu_2SnZn(S,Se)_4$ (CZTSSe) solar cells have promising potential to replace the well-known CIGS ($CuInGaSe_2$) and CdTe solar cells in the long-term not only due to their earth abundant and nontoxic constituents (except Se which has low toxicity and also is readily available) but also due an excellent p type conductivity, a high absorption coefficient ($10^4 cm^{-1}$) and a direct band gap that can be tuned from 1 eV to 3.1 eV by

simply adding or substituting the cation (Sn) with other elements (Ge, Si) or the anion (Se) by S [1]. The narrow region of stability [2] of kesterites leads to the formation of different binary selenides of the constituents elements such as $Cu_x(S,Se)$, Zn(S,Se), $Sn(S,Se)_x$ or $Cu_2Sn(S,Se)_3$ during the processing which dent the performance of the solar cells in varying magnitudes [3,4]. Therefore getting rid of these unwanted phases from the active material is paramount to obtaining good devices. The removal of these secondary phases traditionally requires the use of a wet chemical step. The most widely adapted etching technique for obtaining high efficient CZT(SSe) is the KCN based solution [5,6]. In our previous work [7] we have shown that avoiding the KCN etching step results in less efficient solar cells mainly due to the presence of secondary phases thereby re instating the importance of the KCN immersion step. However, due to persistent problems associated in processing as mentioned earlier the duration and the consequences of KCN etching step also needs some revision and understanding. Ever since IBM reported > 10% efficiencies for CZTSe solar cells [8] with the introduction of a low temperature annealing step in their processing routine it has been used by many groups processing CZTSe devices as a way to improve the efficiency. The reason for this improvement has a variety of perspectives. Among them, the formation of a Cu poor and Zn rich surface and grain boundaries [9] and change in the concentration of Na in the bulk [10] are widely accepted. Since Post deposition Annealing (PDA) is carried out on our samples after full processing to improve solar cell efficiency and not much has been understood even at a qualitative level certain aspects that help in the understanding of the consequences of PDA have also been discussed in this work. Within this framework a few aspects that will enable better understanding of the influence these two steps in processing pure selenide Kesterite CZTSe solar cells have been answered.

2). Experimental Methods

2.1) Processing procedure

All solar cells are fabricated on a 3 mm thick, 25 cm^2 soda lime glass substrate covered by 400 nm of Molybdenum (Mo) as electrical back contact. The constituent elements that make up the absorber layer are deposited in the order Sn/Zn/Cu on top of Mo by electron beam evaporation. The precursor films are then selenized at high temperatures (450ºC) to form crystalline CZTSe thin films. During selenization the sample is held on a square shaped graphite plate to which a thermocouple is connected from the side wall. The temperature is measured from the isolating glass substrate and not from the sample surface. Due to difference in the thermal conductivities one can expect the sample surface to be slightly hotter than the glass substrate. The selenization takes place in a rapid thermal annealing system under a Se rich atmosphere created by a constant flow of H_2Se in the chamber. The absorbers are then immersed in KCN solution (5 wt% in aqueous KOH. The concentration of KOH is 0.5wt% in the KCN solution.) for 30 or 360 seconds to remove secondary phases, elemental selenium and native oxide from the absorber surface. The CdS buffer layer is deposited by chemical bath deposition at 70^o C using $Cd(CH_3CO_2)_2$ and $SC(NH_2)_2$ as precursors in aqueous NH_3 medium. The solar cells were finished by a transparent bi-layer of RF magnetron sputtered i-ZnO (120 nm) and Al:ZnO (280 nm) followed by the deposition of 1 μm thick Al fingers as front contact. Individual cells with an area of 0.5 cm^2 were laterally isolated by mechanical scribing.

2.2) Physical Analysis.

The cross section and chemical composition of the CZTSe thin films used in this study were evaluated by Scanning electron microscope (SEM) Nova 200 FEI tool, equipped with an energy dispersive x ray analysis (EDX) system. The accelerating voltage used for the EDX analysis was 20 kV. X Ray Diffraction (XRD) measurements were carried out on a X' Pert Pro MRD X-ray diffractometer in the conventional Bragg-Brentano ω-2θ geometry using the Cu Kα (1.5418 A˚)

radiation as the incident beam. X ray photoelectron spectroscopy (XPS) measurements were performed using a monochromatized Al Kα X-ray source (1486.6 eV) and a spot size of 400 microns using a Theta300 system in AR-mode. The XPS measurements were performed on identical CZTSe thin film absorbers and not the solar cells that are discussed in the manuscript. For this purpose the tri layer selenization followed by KCN etching (both described previously) were performed on the same day back to back. This was followed by Post deposition Annealing. The Post deposition Annealing step was carried out for 10 minutes at 200°C after which the sample was allowed to cool down to less than 50°C in roughly 15 minutes prior to the XPS measurement of the respective sample. After this the samples were vacuum packed and were taken for measurement.

2.3) Electrical and Optical Analysis.

The processed solar cells were analyzed using Current-Voltage (IV) measurements, using a 2401 Keithley Source meter, under standard test conditions for Kesterite solar cells with a solar simulator system using an AM1.5G spectrum with an illumination density of 1000 W/m^2 at 25°C. The external quantum efficiency (EQE) has been measured at room temperature using a laboratory-built system with a grating monochromator-based dual-beam setup under chopped light from a Xe lamp. The doping profile of the absorbers was measured by capacitance voltage (CV) measurements, which were performed with an Agilent 4980A LCR-meter with frequencies varying from 10 kHz to 100 kHz. The excitation dependent photoluminescence analysis was performed was measured using a Hamamatsu C12132 near infrared compact fluorescence lifetime measurement system equipped with a cryostat that can be cooled down to liquid N_2 (77K) temperatures. The tool uses 15 kHz, 1.2 ns pulsed 532 nm laser and the average laser power was varied between 0.08 mW to 56 mW to illuminate an area of 3 mm diameter on the measured solar cell.

3) Results and discussion.

3.1) Influence of KCN immersion time on CZTSe absorber and solar cells

Figure 1 a) – e) shows the X- SEM Images of CZTSe thin film absorbers with different KCN immersion times. The CZTSe thin film layers were prepared by the selenization of a Sn/Zn/Cu stack as explained in the previous section. The starting precursor composition is [Zn]/[Sn] = 1.07 ± 0.06 and [Cu]/[Zn]+[Sn] = 0.69 ± 0.03. The absorber thickness is somewhat higher in the case of the sample that had no KCN immersion compared to the others. (The absorber thickness was calculated from the SEM pictures with the micro marker from 5 different places and averaged). The average thickness of the absorber for no KCN immersion is 1.25µm whereas for the 360 seconds KCN immersed absorber it is 1.04µm. Suspecting a certain removal of mass from the thin films during the etching process standard mass measurements were carried out using a conventional mass balance in the laboratory. The least count of the balance used is 10^{-5} grams. The data reported in this figure was obtained from the same absorber. The first point in the y axis for 0s (no etching) is the difference in mass between the CZTSe thin film absorber on Mo/SLG after selenization and bare Mo/SLG. The remaining points in the y axis represent the difference between the CZTSe absorbers immersed in KCN for various times and the CZTSe absorber not subjected to KCN etching. Hence, the reported mass change is positive. From figure 1f) we see that with the increase in the immersion time the measured mass increases steadily up to 240s and marginally up to 360s and shows no change thereafter. Taking into account the change in mass, the initial thickness and atomic density of CZTSe the removal of mass after 360 seconds of KCN immersion corresponds to a thickness of 190 nm which is in agreement with the X - SEM Images. The physical meaning behind this was understood from the analysis of XRD and SEM-EDX measurements shown in figure 1g) and 1h). XRD patterns revealed that the selenized absorber contains small amounts of CuSe, SnSe and $SnSe_2$ secondary phases [11]. KCN immersion up to 120 seconds appears to etch away most of these secondary phases. The cation ratios measured by EDX vary within this time.

The [Cu]/[Zn]+[Sn] ratio which is initially 0.71 before KCN immersion increases to 0.78 after 120 seconds due to removal of Cu and Sn related secondary phases whereas [Zn]/[Sn] ratio climbs from 1.14 to 1.25 strongly due to the removal of Sn related phases. Above 120 seconds the [Cu]/[Zn]+[Sn] ratio drops to 0.76 and [Zn]/[Sn] ratio drops to 1.22. Change in the ratios above 120s of KCN immersion cannot be explained by secondary phases. Correlating this information with the data obtained from mass measurements it can be concluded that longer immersion times of CZTSe in KCN based solution (5 wt% in aqueous KOH in this case) might result in preferential etching of CZTSe itself preferably from the free surfaces exposed to the solution. In a previous work it was shown that when the KCN (same conc.) duration was varied for Cu poor, Zn rich CZTSe absorbers the preferential etching of the elements during long immersion times is due to KOH in the solution mix. This was explained due to the presence of stable hydroxide-based complex ions with Sn and Zn, which can be easily formed because of their relatively high oxidation states in CZTSe (+IV and +II for Sn and Zn, respectively) compared to Cu (+I) [12].

Figure 2a) shows the efficiencies of the solar cells with different KCN immersion times .The solar cell "0s" (no KCN immersion) has the lowest average efficiency (2.15 ± 0.55)% in the series. The IV measurements were performed on solar cells fabricated on a 2.5 x 5 cm^2 Mo/SLG substrate. After full solar cell processing (including grids) each sample had 8 – 10 functional cells with an area of 0.5 cm^2. Best IV parameters were obtained for the solar cell with 120s (5.66 ± 0.44) % of KCN etching with a champion efficiency of 6.1%. An immersion time above 120 seconds resulted in degradation of efficiencies primarily due to the decrease in fill factor (FF) and low short circuit currents (J_{sc}'s).Figure 2b) shows the doping profile of the solar cells deduced from CV measurements. It can be seen that the doping of the CZTSe absorber increases roughly by 1 order of magnitude when increasing the immersion time in the KCN/KOH solution from 0 to 360 s, thereby decreasing the apparent space charge region (SCR) width in the absorber.

The change in doping density could also be due to the modification of the content of alkali elements by the KCN solution in the CZTSe absorber [12]. The external quantum efficiency (EQE) curves of these solar cells shown in figure 2c) measured without light bias reveal that the maximum EQE value (at 520 nm) increases up to 120s of treatment, and decreases abruptly for longer immersion times. This wavelength corresponds to photons generated near the CdS/CZTSe interface. The evolution of the EQE curves for longer immersion times can be due to the modification of the SCR width or an unfriendly band alignment e.g "spike" like band offset between CdS and CZTSe [13] resulting in poor carrier collection. Temperature dependent IV measurements show that the extrapolation of the Open circuit voltage (V_{oc}) progressively decreases as the etching duration increases from 30s to 360s, implying that the main location of the limiting recombination mechanism is moving from bulk to interface. Considering the findings from physical and electrical analysis of the absorber and the solar cells the loss of FF of the devices with longer immersion times is expected to be a consequence of the preferential etching of Se, Sn, and Zn from the CZTSe surface by the KOH solution (maybe) in combination with an interface barrier which arises due to the systematic damage of the free surface of CZTSe.

3.2 Effect of Post deposition Annealing.

The CZTSe solar cells seen in the previous section were annealed in N_2 atmosphere at 200ºC for 10 minutes. The performance of the solar cells after annealing is shown in figure 3b) in comparison with the figure 3a) without annealing. The annealing has resulted in degradation of the good devices (30s and 120s) and has also improved the poor devices (0s, 240s & 360s). For the purpose of discussion solar cells without annealing will be referred as "As processed" (**AP**) and solar cells annealed will be referred as " Post deposition annealed" (**PDA**).

In order to understand what the annealing might have done to the CZTSe solar cells , a solar cell (6.1%) which suffered degradation (4.7%, case **A**) after PDA and a solar cell (2.7%) which improved (5.2%, case **B**) after PDA were analyzed in more detail. Figure 4 a) show small changes in the doping density and c) shows reduced carrier collection in the visible region for case **A** after PDA. The decrease in the band gap of CZTSe (seen from PL inset) after PDA could be related to an increase in the disorder of CZTSe [14], whereas for case **B** after PDA there is a change in the magnitude of doping density by an order leading to a wider SCR width (Fig.4 c) in the CZTSe. This is also reflected in the enhanced carrier collection in this device (Fig. 4 d). However, there is no change in the band gap. The real reason for no change in the band gap of the 2.7 % cell is not known and it is beyond the scope of this work to understand that. Therefore it is safe to say that the change in the device performance after PDA might not be necessarily related only with the order - disorder transitions reported for Kesterites.

To understand further, excitation dependent PL analysis was conducted on these 4 devices. The recombination dynamics for CZTSe explained by the Quasi Donor to Acceptor Model (Q-DAP) was best suited for these absorbers as well. Using the concepts and equations explained by Gershon et al. [15] the Q - DAP pair density was calculated for all 4 devices. The Q - DAP density was plotted against the V_{oc} of these devices as shown in Fig.4 e). From the plot it is clear that higher defect densities were accompanied with a low V_{oc} and vice versa. Larger defect densities can result in the reduction of V_{oc} (via formation of tail states) [16] thereby explaining the change in the device performance which also clearly illustrates that PDA modifies the bulk defect density of the CZTSe absorber.

Since few reports [17], discuss surface related compositional changes after PDA, XPS measurements were performed to observe similar changes. The procedure for performing the measurements has been explained in the methods section. The absorbers without and with KCN immersion show a significant change in the measured oxygen content and it keeps reducing with increased immersion time which could be most likely due to removal of native oxide from the surface by KCN/KOH solution.

However, there is no trend in the oxygen content measured by XPS and the device efficiency. Alkali elements (Na and K) were also not detected by XPS. Hence, these results are not shown. The relative concentration of the cations at the surface of the absorber has been plotted against the condition of the solar cell (Fig.4f).In case **A**, it can be seen that after PDA at the surface Cu decreases, Sn increases & Zn does not change resulting in a Cu depleted and Sn rich conditions at the surface whereas in case **B**, the change in concentrations result in Cu depleted and Zn rich conditions. Thus PDA can result in the movement of the cations away from and towards the surface. However, when there is Cu diffusion towards bulk and Zn diffusion towards the surface forming a Cu poor, Zn rich surface creation of [V_{Cu} +Zn_{Cu}] defect clusters in surface region will take place [9].The Formation of [V_{Cu}+Zn_{Cu}] defect pairs on surface has been reported to be beneficial for junction formation and device performance [18]. This could be one of the reasons that explains the improvement of the 2.7% device after PDA. The XPS measurements were performed on CZTSe absorbers identical to the ones discussed thus far. The purpose of these measurements is to verify whether surface related composition changes take place or not in the absorber after PDA. Hence strict correlations between the surface related composition changes and the device performance after PDA are not attempted.

4) Conclusions

Overall a KCN immersion step is required to make CZTSe devices with optimum efficiencies at least for our samples. When a KCN solution along with KOH is used in the immersion step then it is best to limit the duration to below 240 seconds as further immersion would result in the degradation of CZTSe affecting both the bulk and the interface which results in poor solar cell poor efficiencies. Involving an annealing step in the processing does not always result in the improvement of efficiencies. The extent of changes (defect density, composition changes) caused by annealing in the bulk and at the surface of the absorber could determine the performance of the solar cell.

Acknowledgements

This research is partially funded by the Flemish government, Department Economy, Science and innovation. This research has received funding from the European Union's Horizon 2020 research and innovation program under grant agreement No 640868.

References:

[1] D. B. Khadka, J. Kim, Band Gap Engineering of Alloyed $Cu_2ZnGe_xSn_{1-x}Q_4$ (Q=S,Se) Films for Solar CellJ. Phys. Chem. C 119, *(***2015)**, 1706

[2] Olekseyuk, I. D., Dudchak, I. V. & Piskach, L. V. Phase equilibria in the Cu_2S-ZnS-SnS_2 system. Journal of Alloys and Compounds, **368** (1–2), (2004) 135–143.

[3] T. Tanaka, T. Sueishi , K. Saito, Q. Guo, M. Nishio, K.Yu, V. Walukiewicz , Existence and Removal of Cu2Se Second Phase in Co evaporated Cu2ZnSnSe4 Thin Films. J. Appl. Phys. 111,(2012),053522.

[4] G. Brammertz, S. Oueslati, M. Buffière, J. Bekaert, H. ElAnzeery, K.B. Messaoud, S. Sahayaraj, T. Nuytten, C. Koble, M. Meuris, J. Poortmans, Investigation of Properties Limiting Efficiency in Cu2ZnSnSe4 based Solar Cells. IEEE J. Photovoltaics 5, (2015), 649 − 655

[5] S. Oueslati, G. Brammertz, M. Buffière, H. ElAnzeery, O.Touayar, C. Köble, J.Bekaert, M. Meuris, J. Poortmans, Physical and Electrical Characterization of High-Performance Cu2ZnSnSe4 based Thin Film Solar Cells. Thin Solid Films 582, (2015) 224−228

[6] J. Jeon, K.D. Lee, L.S. Oh, S.W. Seo, D.K. Lee, H. Kim, J.H. Jeong, M.J. Ko, B. Kim, H.J. Son, J.Y. Kim, Highly Efficient Copper-Zinc-Tin-Selenide (CZTSe) Solar Cells by Electrodeposition. Chem Sus Chem 4, (2014) 1073−1077.

[7] S. Sahayaraj, G. Brammertz, M. Buffi`ere, M. Meuris, J. Vleugels, J. Poortmans, Effect of Cu content and temperature on the properties of $Cu_2ZnSnSe_4$ solar cells, EPJ Photovoltaics (accepted for publication).

[8] K. Sardashti, R. Haight, T. Gokmen, W. Wang, L.Y. Chang, D.B. Mitzi, A.C. Kummel, Impact of Nanoscale Elemental Distribution in High-Performance Kesterite Solar Cells. Adv. Energy Mater. 5, (2015), 1402180.

[9] M. Neuschitzer, Y. Sanchez, T. Olar, T. Thersleff, S. Lopez-Marino, F. Oliva, M. Espindola-Rodriguez, H. Xie, M. Placidi, V. Izquierdo-Roca, I. Lauermann, K. Leifer, A. Pérez-Rodriguez, E.Saucedo, Complex Surface Chemistry of Kesterites: Cu/Zn Reordering after Low Temperature Postdeposition Annealing and Its Role in High Performance Devices. Chem. Mater. 27, (2015), 5279−5287.

[10] D. Hironiwa, N. Sakai, T. Kato, H. Sugimoto, Z. Tang, J. Chantana, T. Minemoto, Impact of Annealing Treatment before Buffer Layer Deposition on $Cu_2ZnSn(S,Se)_4$ Solar Cells. Thin Solid Films 582, (2015), 151−153.

[11] International Center for Diffraction Data: CZTSe – 04-010-6295; SnSe : 04-009-2274; $SnSe_2$: 01-089-2939; CuSe:00-049-1456; Cu1.8Se:04-004-4729;Cu_2Se:00-029-0575; Mo – 01-088-2331.

[12] M. Buffière, G. Brammertz, S.Sahayaraj, M.Batuk, S. Khelifi, D.Mangin, A.A El Mel, L. Arzel, J. Hadermann, M. Meuris and J.Poortmans. KCN Chemical Etch for Interface Engineering in $Cu_2ZnSnSe_4$ Solar Cells ACS Appl. Mater. Interfaces 7, (2015), **14690**.

[13] R. Haight , A. Barkhouse, O. Gunawan, B. Shin, M. Copel, M. Hopstaken, & D.B. Mitzi, Band alignment at the $Cu_2ZnSn(Sx Se1–x)_4$/CdS interface. *Applied Physics Letters*, **98**, (2011), 253502.

[14] G. Rey, A. Redinger, J. Sendler, T. P. Weiss, M. Thevenin, M. Guennou, B. El Adib, and S. Siebentritt. The band gap of $Cu_2ZnSnSe_4$: Effect of order-disorder. Applied Physics Letters **105**, (2014), 112106.

[15] T. Gershon, B. Shin, N. Bojarczuk, T.Gokmen, S.Lu, and S. Guha, Photoluminescence characterization of a high-efficiency Cu_2ZnSnS_4 device. Journal of Applied Physics **114**, (2013), 154905.

[16] T. Gokmen, O. Gunawan, T. K. Todorov, and D. B. Mitzi, Relationship between Cu2ZnSnS4 quasi donor-acceptor pair density and solar cell efficiency. Appl. Phys. Lett. 103, (2013),103506.

[17] H.Xie, S.López-Marino, T.Olar, Y. Sánchez, M. Neuschitzer, F.Oliva, S.Giraldo, V. Izquierdo-Roca, I. Lauermann, A. Pérez- Rodríguez and E. Saucedo, Impact of Na Dynamics at the $Cu_2ZnSn(S,Se)_4$/CdS Interface During Post Low Temperature Treatment of Absorbers. ACS Appl. Mater. Interfaces 8, (2016), 5017−5024.

[18] S. Chen, A. Walsh, X. Gao Gong , and S.H. Wei. Classification of Lattice Defects in the Kesterite Cu_2ZnSnS_4 and $Cu_2ZnSnSe_4$ Earth-Abundant Solar Cell Absorbers. Adv. Mater. 25, (2013), 1522–1539.

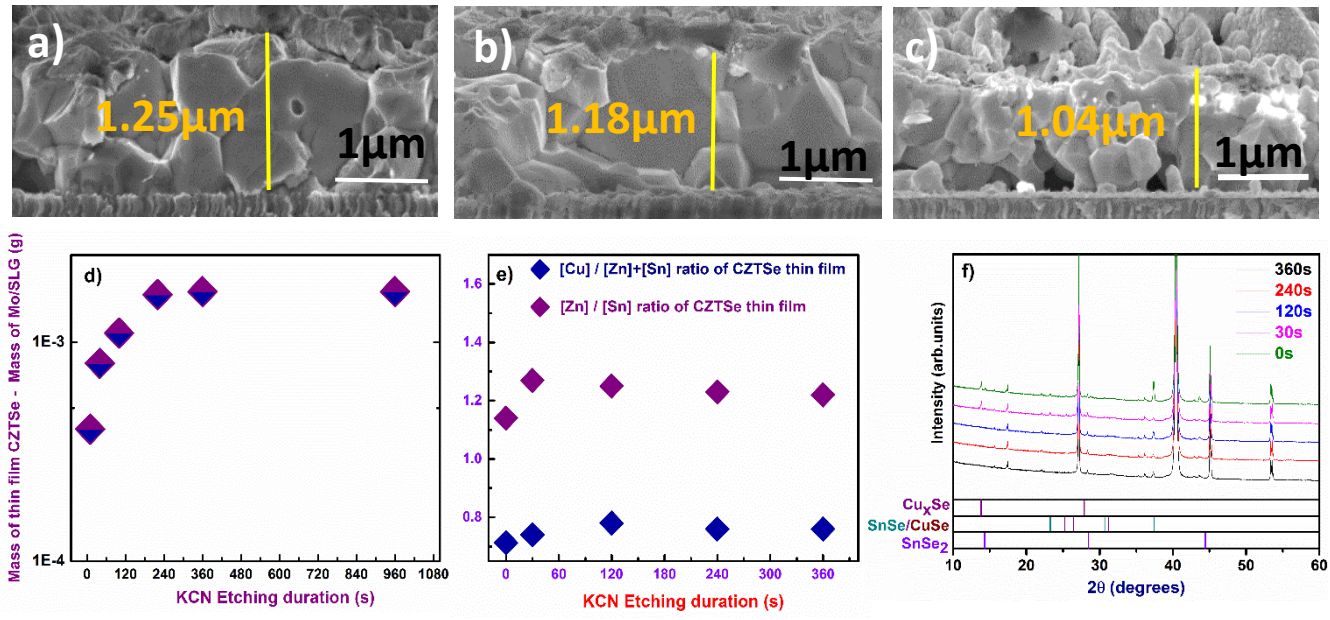

Figure 1 X- SEM Images of CZTSe thin film with a) no KCN immersion step. b) & c) immersed in KCN for 120s and 360s. d) Mass of material removed from CZTSe thin film as a function of KCN immersion time. e) Cation ratios of CZTSe thin films as a function of different KCN immersion times measured by SEM – EDX. f) XRD patterns of CZTSe thin films as a function of KCN immersion time.

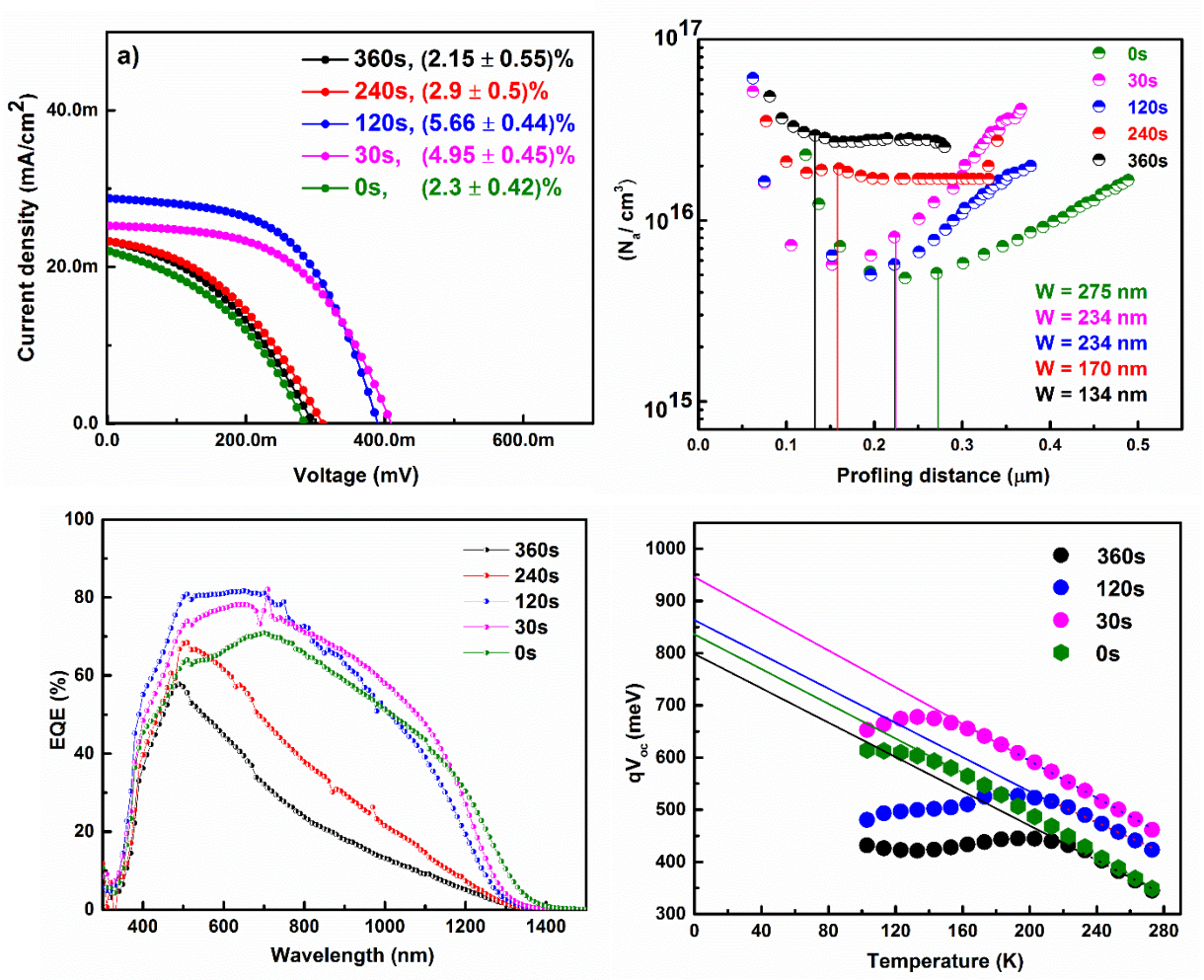

Figure 2 a) Illuminated IV curves under AM 1.5G spectrum b) Doping density as a function of the profiling distance from the p-n junction for different KCN immersion times c) External quantum efficiency (EQE) curves for solar cells with different KCN immersion times d) Plot of Voc vs Temperature deduced form temperature dependent IV measurements as a function of KCN immersion time.

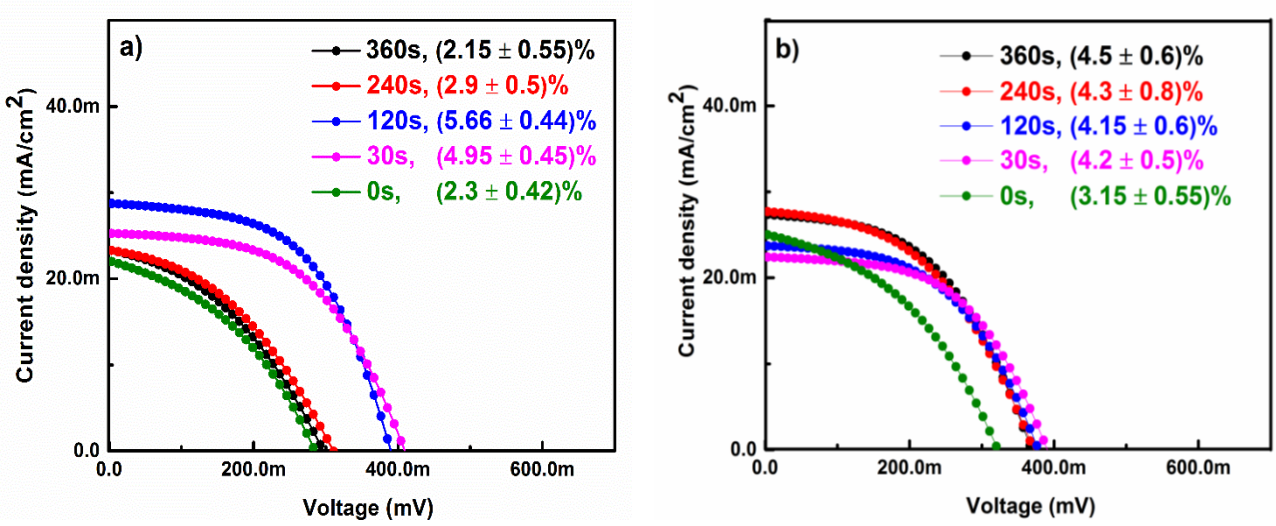

Figure 3 a) Illuminated IV curves under AM 1.5G spectrum before annealing at 200ºC b) Illuminated IV curves under AM 1.5G spectrum after annealing at 200ºC

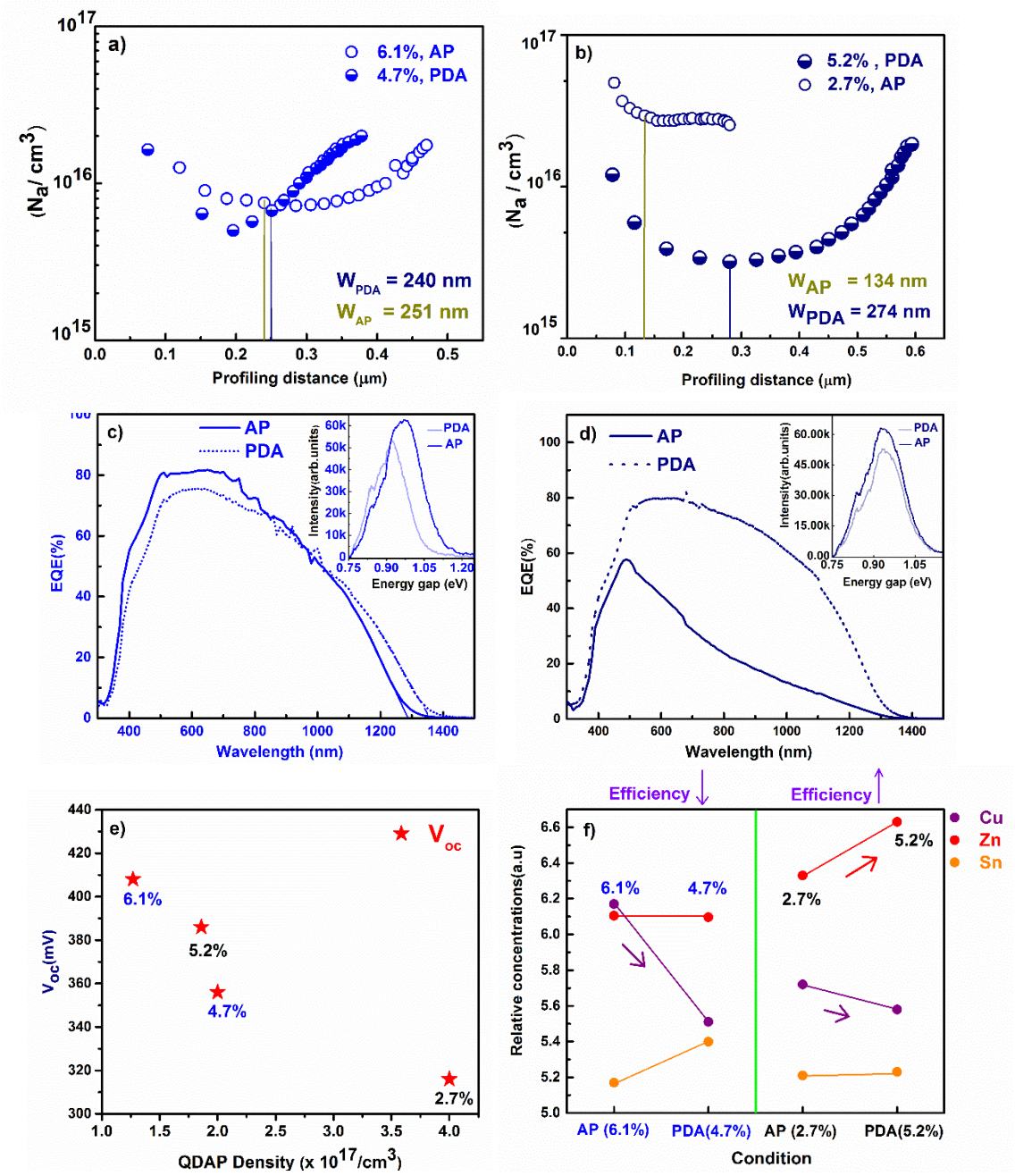

Figure 4 a) & c) Doping profile extracted from CV and EQE spectrum before and after annealing for the degraded device b) & d)) Doping profile extracted from CV and EQE spectrum before and after annealing for the improved device e) Plot of Q- DAP density of the p type absorber vs Voc f) XPS measurements showing the cation composition at the surface before and after annealing for two cases.